Mean-Variance Analysis
in Bayesian Optimization under Uncertainty

Shogo Iwazaki
Nagoya Institute of Technology

Yu Inatsu
Nagoya Institute of Technology

Ichiro Takeuchi
Nagoya Institute of Technology
RIKEN
takeuchi.ichiro@nitech.ac.jp

Abstract

We consider active learning (AL) in an uncertain environment in which trade-off between multiple risk measures need to be considered. As an AL problem in such an uncertain environment, we study Mean-Variance Analysis in Bayesian Optimization (MVA-BO) setting. Mean-variance analysis was developed in the field of financial engineering and has been used to make decisions that take into account the trade-off between the average and variance of investment uncertainty. In this paper, we specifically focus on BO setting with an uncertain component and consider multi-task, multi-objective, and constrained optimization scenarios for the mean-variance trade-off of the uncertain component. When the target blackbox function is modeled by Gaussian Process (GP), we derive the bounds of the two risk measures and propose AL algorithm for each of the above three scenarios based on the risk measure bounds. We show the effectiveness of the proposed AL algorithms through theoretical analysis and numerical experiments.

1 Introduction

Decision making in an uncertain environment has been studied in various domains. For example, in financial engineering, the mean-variance analysis (Markowitz, 1952; Markowitz and Todd, 2000; Keeley and Furlong, 1990) has been introduced as a framework for making investment decisions, taking into account the trade-off

between the return (mean) and the risk (variance) of the investment. In this paper we study active learning (AL) in an uncertain environment. In many practical AL problems, there are two types of parameters called *design parameters* and *environmental parameters*. For example, in a product design, while the design parameters are fully controllable, the environmental parameters vary depending on the environment in which the product is used. In this paper, we examine AL problems under such an uncertain environment, where the goal is to efficiently find the optimal design parameters by properly taking into account the uncertainty of the environmental parameters.

Concretely, let $f(\boldsymbol{x}, \boldsymbol{w})$ be a blackbox function indicating the performance of a product, where $\boldsymbol{x} \in \mathcal{X}$ is the set of controllable design parameters and $\boldsymbol{w} \in \Omega$ is the set of uncontrollable environmental parameters whose uncertainty is characterized by a probability distribution $p(\boldsymbol{w})$. We particularly focus on the AL problem where the mean and the variance of the environmental parameters,

$$\mathbb{E}_{\boldsymbol{w}}[f(\boldsymbol{x}, \boldsymbol{w})] = \int_{\Omega} f(\boldsymbol{x}, \boldsymbol{w}) p(\boldsymbol{w}) \mathrm{d}\boldsymbol{w}, \tag{1a}$$

$$\mathbb{V}_{\boldsymbol{w}}[f(\boldsymbol{x}, \boldsymbol{w})] = \int_{\Omega} (f(\boldsymbol{x}, \boldsymbol{w}) - \mathbb{E}_{\boldsymbol{w}}[f(\boldsymbol{x}, \boldsymbol{w})])^2 p(\boldsymbol{w}) \mathrm{d}\boldsymbol{w}, \tag{1b}$$

respectively, are taken into account. Specifically, we work on these two measures in three different scenarios: multi-task learning scenario, multi-objective optimization scenario, and constrained optimization scenario. In the first scenario, we study one of multi-task formulations in which a weighted sum of these two measures is maximized [1]. In the second scenario, we discuss how to obtain the Pareto frontier of these two measures in an AL setting. In the third scenario, we consider optimizing one of the two measures under some constraint on the other measure. We refer to

---

[1]This formulation is also referred as a scalarization objective in multi-objective optimization.

these problems and the proposed framework for solving them as *Mean-Variance Analysis in Bayesian Optimization (MVA-BO)*. Figure 1 shows an illustration of a multi-task learning scenario.

In this study, we employ a Gaussian process (GP) to model the uncertainty of the blackbox function $f(\boldsymbol{x}, \boldsymbol{w})$. In a conventional GP-based AL problem (without uncontrollable environmental parameters $\boldsymbol{w}$), the acquisition function (AF) is designed based on how the uncertainty of the blackbox function changes when an input point is selected and the blackbox function is evaluated. On the other hand, in MVA-BO, we need to know how the uncertainties of the mean function (1a) and the variance function (1b) change by evaluating the blackbox function at the selected input point. Note that we face the difficulty of not being able to directly evaluate the target functions (1a) and (1b). It has been shown in a previous study (O'Hagan, 1991) that, when $f(\boldsymbol{x}, \boldsymbol{w})$ follows a GP, the mean function (1a) also follows a GP. Unfortunately, however, the variance function (1b) does not follow a GP, indicating that we need to develop a new method to quantify how the uncertainty of the variance function changes by evaluating the blackbox function at the selected input point. In this study, we extend the GP-UCB algorithm (Srinivas et al., 2010) to realize MVA-BO in the above mentioned three scenarios by overcoming these technical difficulties. We demonstrate the effectiveness of the proposed MVA-BO framework through theoretical analyses and numerical experiments.

Related Work   Various problem setups and methods have been studied for AL and Bayesian optimization (BO) problems when there are multiple target functions. One of such problem setup is multi-task BO (Swersky et al., 2013). In this problem setup, the AF is designed to select input points that commonly contribute to optimizing multiple target functions. Another popular problem setup is multi-objective BO (Emmerich, 2005; Zuluaga et al., 2016; Suzuki et al., 2020). The goal of a multi-objective optimization is to obtain so-called *Pareto-optimal* solutions. The AF in this problem setup is designed to efficiently identify solutions on the Pareto frontier. Another common problem setup is constrained BO (Gardner et al., 2014; Gelbart et al., 2014; Hernández-Lobato et al., 2016; Takeno et al., 2021). The goal of this problem setup is to find the optimal solution to a constrained optimization problem in a situation where both the objective function and constraint function are blackbox functions that are costly to evaluate. The AF in this problem setup is designed to select input points that are useful not only for maximizing the objective function but also for identifying the feasible region. In this paper, we study these three scenarios as concrete examples of MVA-BO. Unlike conventional multi-task, multi-objective and constrained BOs, the main technical challenges of MVA-BO are that the two target functions (1a) and (1b) cannot be directly evaluated and that the latter does not follow a GP.

Various studies have been published on BO under various types of uncertainty. The most relevant one to our study is on *Bayesian quadrature optimization (BQO)* (Toscano-Palmerin and Frazier, 2018), the goal of which is to optimize the mean function (1a). When the blackbox function follows a GP, the mean function (1a) also follows a GP, suggesting that one can efficiently solve BQO problems by properly modifying the AFs in conventional BO. By replacing the integrand in (1a) with different measures, one can consider various types of AL problems under uncertainty (Beland and Nair, 2017; Iwazaki et al., 2020a,b; Cakmak et al., 2020). Another line of research dealing with uncontrollable and uncertain factors in BO is known as *robust BO* (Bogunovic et al., 2018; Nguyen et al., 2020; Kirschner et al., 2020; Bogunovic et al., 2020; Inatsu et al., 2021). The goal of robust BO is to make robust decisions that appropriately take into account various types of uncertainty. For example, input uncertainty in BO has been studied, in which probabilistic noise is inevitably added to the input points when evaluating the target blackbox function. Although research on BO in an uncertain environment has steadily progressed over the past few years, to our knowledge, there are no AL nor BO studies that take into account the trade-offs between multiple measures such as mean-variance analysis.

Decision making under uncertainty is being examined in the field of robust optimization (Ben-Tal et al., 2009; Beyer and Sendhoff, 2007; Ben-Tal and Nemirovski, 2002), with especially applications to financial engineering in mind (Schied, 2006; Alexander and Baptista, 2002; Fabozzi et al., 2007). It has been pointed out that when making decisions under uncertainty, it is important to balance multiple measures appropriately, as represented by the Nobel prize-winning mean-variance analysis in portfolio theory (Markowitz, 1952; Markowitz and Todd, 2000; Keeley and Furlong, 1990). Various risk measures, such as Value at Risk (VaR), have been proposed in financial engineering, and these multiple risk measures are used in combination, depending on the purpose of the decision making. However, to our knowledge, there have not been AL or BO studies that have appropriately taken into account multiple measures.
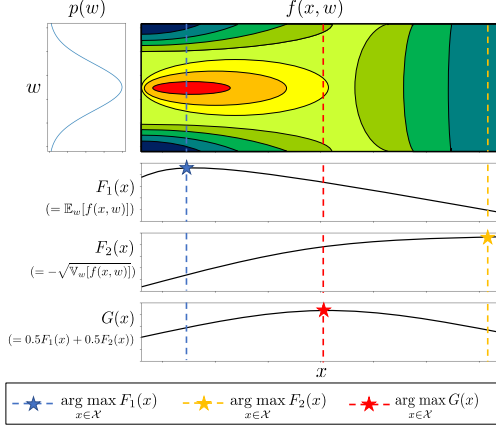
Shogo Iwazaki, Yu Inatsu, Ichiro Takeuchi

Figure 1: 2D synthetic example under a multi-task scenario. The horizontal and vertical axes represent the design and environmental parameters $\boldsymbol{x}$ and $\boldsymbol{w}$, respectively. Blue and yellow dotted lines indicate the points where expected value $F_1(\boldsymbol{x})$ and negative standard deviation $F_2(\boldsymbol{x})$ of $f(\boldsymbol{x}, \boldsymbol{w})$ are maximum. Our goal is to identify the point on the red line that simultaneously maximize both of F_1 and F_2 .

2 Preliminaries

2.1 Problem Setup

Let $f : \mathcal{X} \times \Omega \to \mathbb{R}$ be a blackbox function which is expensive to evaluate, where $\mathcal{X}$ and Ω are a finite set [2] and a compact convex set, respectively. We assume that a variable $\boldsymbol{w} \in \Omega$ is probabilistically fluctuated by a known density function $p(\boldsymbol{w})$ [3]. At every step t, a user selects the next input point $\boldsymbol{x}_t \in \mathcal{X}$, whereas $\boldsymbol{w}_t \in \Omega$ will be given as a realization of the random variable. Next, the user gets a noisy observation $y_t = f(\boldsymbol{x}_t, \boldsymbol{w}_t) + \eta_t$, where η_t is independent Gaussian noise from $\mathcal{N}(0, \sigma^2)$.

Throughout the paper, we assume that f is an element of reproducing kernel Hilbert space (RKHS) and has a bounded norm (Srinivas et al., 2010). Let k be a positive definite kernel with $\forall (\boldsymbol{x}, \boldsymbol{w}) \in (\mathcal{X} \times \Omega), k((\boldsymbol{x}, \boldsymbol{w}), (\boldsymbol{x}, \boldsymbol{w})) \leq 1$, and $\mathcal{H}_k$ be an RKHS corresponding to k. In this paper, for some positive constant B, we assume $f \in \mathcal{H}_k$ with $\|f\|_{\mathcal{H}_k} \leq B$, where $\| \cdot \|_{\mathcal{H}_k}$ denotes the Hilbert norm defined on $\mathcal{H}_k$.

Models Our algorithm is built on a GP model (Rasmussen and Williams, 2006). First, we assume

---

[2] We discuss the case where $\mathcal{X}$ is a continuous set in Appendix C.

[3] A probability mass function can be similarly considered when Ω is a finite set. In that case, the subsequent discussions still hold if integral operations are replaced by summation operations.

$\mathcal{GP}(0, k)$ as a prior of f, where $\mathcal{GP}(\mu, k)$ is a GP characterized by a mean function μ and a kernel function k. Given a sequence of instances $\{((\boldsymbol{x}_i, \boldsymbol{w}_i), y_i)\}_{i=1}^t$, the posterior distribution of $f(\boldsymbol{x}, \boldsymbol{w})$ is the Gaussian distribution with the mean and the variance defined as follows:

$$\mu_t(\boldsymbol{x}, \boldsymbol{w}) = \boldsymbol{k}_t(\boldsymbol{x}, \boldsymbol{w})^\top \left(\boldsymbol{K}_t + \sigma^2 \boldsymbol{I}_t \right)^{-1} \boldsymbol{y}_t,$$
$$\sigma_t^2(\boldsymbol{x}, \boldsymbol{w}) = k \left((\boldsymbol{x}, \boldsymbol{w}), (\boldsymbol{x}, \boldsymbol{w}) \right)$$
$$- \boldsymbol{k}_t(\boldsymbol{x}, \boldsymbol{w})^\top \left(\boldsymbol{K}_t + \sigma^2 \boldsymbol{I}_t \right)^{-1} \boldsymbol{k}_t(\boldsymbol{x}, \boldsymbol{w}),$$

where $\boldsymbol{k}_t(\boldsymbol{x}, \boldsymbol{w}) \in \mathbb{R}^t$ is a vector whose i^{th} element is $k((\boldsymbol{x}, \boldsymbol{w}), (\boldsymbol{x}_i, \boldsymbol{w}_i))$, $\boldsymbol{I}_t$ is the identity matrix of size t, and $\boldsymbol{K}_t$ is the $t \times t$ kernel matrix whose $(i, j)^{\text{th}}$ element is $k((\boldsymbol{x}_i, \boldsymbol{w}_i), (\boldsymbol{x}_j, \boldsymbol{w}_j))$.

We use the quantity called maximum information gain, which is often used in the standard GP-based optimization literatures (Srinivas et al., 2010; Chowdhury and Gopalan, 2017). The maximum information gain at step t is defined as

$$\gamma_t = \max_{\boldsymbol{x}_1, \dots, \boldsymbol{x}_t} \frac{1}{2} \ln \det(\boldsymbol{I}_t + \sigma^{-2} \boldsymbol{K}_t).$$

Finally, we introduce the following lemma to construct the confidence bound of f based on the posterior mean μ_t and the variance σ_t^2.

Lemma 2.1. *Fix $f \in \mathcal{H}_k$ with $\|f\|_{\mathcal{H}_k} \leq B$. Given $\delta \in (0, 1)$, let $\beta_t = \left(\sqrt{2(\gamma_{t-1} + \ln 1/\delta)} + B \right)^2$. Then, with probability at least $1 - \delta$, for any $\boldsymbol{x} \in \mathcal{X}$, $\boldsymbol{w} \in \Omega$, $t \geq 1$,*

$$|f(\boldsymbol{x}, \boldsymbol{w}) - \mu_{t-1}(\boldsymbol{x}, \boldsymbol{w})| \leq \beta_t^{1/2} \sigma_{t-1}(\boldsymbol{x}, \boldsymbol{w}). \quad (2)$$

This lemma is easily derived by combining the definition of γ_t and Theorem 3.11 in Abbasi-Yadkori (2013). Based on Lemma 2.1, the confidence bound $Q_t(\boldsymbol{x}, \boldsymbol{w}) := [l_t(\boldsymbol{x}, \boldsymbol{w}), u_t(\boldsymbol{x}, \boldsymbol{w})]$ of $f(\boldsymbol{x}, \boldsymbol{w})$ can be computed by

$$l_t(\boldsymbol{x}, \boldsymbol{w}) = \mu_{t-1}(\boldsymbol{x}, \boldsymbol{w}) - \beta_t^{1/2} \sigma_{t-1}(\boldsymbol{x}, \boldsymbol{w}),$$
$$u_t(\boldsymbol{x}, \boldsymbol{w}) = \mu_{t-1}(\boldsymbol{x}, \boldsymbol{w}) + \beta_t^{1/2} \sigma_{t-1}(\boldsymbol{x}, \boldsymbol{w}).$$

2.2 Target Functions and Scenarios

We consider the expectation and variance of $f(\boldsymbol{x}, \boldsymbol{w})$ under the uncertainty of $p(\boldsymbol{w})$ as (1a) and (1b) in §1. Using $\mathbb{E}_{\boldsymbol{w}}[f(\boldsymbol{x}, \boldsymbol{w})]$ and $\mathbb{V}_{\boldsymbol{w}}[f(\boldsymbol{x}, \boldsymbol{w})]$, we define the following target functions F_1 and F_2:

$$F_1(\boldsymbol{x}) = \mathbb{E}_{\boldsymbol{w}}[f(\boldsymbol{x}, \boldsymbol{w})], \ F_2(\boldsymbol{x}) = -\sqrt{\mathbb{V}_{\boldsymbol{w}}[f(\boldsymbol{x}, \boldsymbol{w})]}. \quad (3)$$

We consider these two functions as the targets of decision making processes in the following three scenarios.

Multi-task (MT)-Scenario First, we formulate the problem as a single-objective optimization problem whose objective function is defined as a weighted sum of F_1 and F_2. Given a user-specified weight $\alpha \in [0,1]$, let G be a new objective function defined as

$$G(\boldsymbol{x}) = \alpha F_1(\boldsymbol{x}) + (1-\alpha)F_2(\boldsymbol{x}).$$

Here, the goal is to find $\boldsymbol{x}^* \coloneqq \operatorname{argmax}_{\boldsymbol{x} \in \mathcal{X}} G(\boldsymbol{x})$ efficiently. For analyzing the theoretical properties, we introduce the notion of an ϵ-*accurate solution*. Let $\hat{\boldsymbol{x}}_t$ be an estimated solution obtained by the algorithm at step t. Given a fixed constant $\epsilon \geq 0$, we say that $\hat{\boldsymbol{x}}_t$ is ϵ-*accurate* if the following inequality holds:

$$G(\hat{\boldsymbol{x}}_t) \geq G(\boldsymbol{x}^*) - \epsilon.$$

In §4, for an arbitrarily small ϵ, we show that our algorithm can find an ϵ-accurate solution with high probability after finite step T.

Multi-objective (MO)-Scenario We also consider another formulation based on the Pareto optimality criterion. Hereafter, we use the vector representation of the objective functions: $\boldsymbol{F}(\boldsymbol{x}) = (F_1(\boldsymbol{x}), F_2(\boldsymbol{x}))$. First, let $\preceq$ be a relational operator defined over $\mathcal{X} \times \mathcal{X}$ or $\mathbb{R}^2 \times \mathbb{R}^2$. Given $\boldsymbol{x}, \boldsymbol{x}' \in \mathcal{X}$, we write $\boldsymbol{x} \preceq \boldsymbol{x}'$ or $\boldsymbol{F}(\boldsymbol{x}) \preceq \boldsymbol{F}(\boldsymbol{x}')$ provided that $F_1(\boldsymbol{x}) \leq F_1(\boldsymbol{x}')$ and $F_2(\boldsymbol{x}) \leq F_2(\boldsymbol{x}')$ hold simultaneously. An operator $\prec$ is similarly defined.

The goal of this scenario is to identify the following *Pareto set* Π efficiently:

$$\Pi = \{\boldsymbol{x} \in \mathcal{X} \mid \forall \boldsymbol{x}' \in E_{\boldsymbol{x}}, \boldsymbol{F}(\boldsymbol{x}) \npreceq \boldsymbol{F}(\boldsymbol{x}')\},$$

where $E_{\boldsymbol{x}} = \{\boldsymbol{x}' \in \mathcal{X} \mid \boldsymbol{F}(\boldsymbol{x}) \neq \boldsymbol{F}(\boldsymbol{x}')\}$. Moreover, *Pareto front* Z is defined by

$$Z = \partial\{\boldsymbol{y} \in \mathbb{R}^2 \mid \exists \boldsymbol{x} \in \mathcal{X}, \boldsymbol{y} \preceq \boldsymbol{F}(\boldsymbol{x})\},$$

where ∂A denote the boundary of the set A.

Next, we introduce the notion of an ϵ-accurate Pareto set (Zuluaga et al., 2016), which is an idea similar to the ϵ-accurate solution in the multi-task scenario. Given a non-negative vector $\boldsymbol{\epsilon} = (\epsilon_1, \epsilon_2)$, we define the relational operator $\preceq_{\boldsymbol{\epsilon}}$, which is the relaxed version of $\preceq$. For $\boldsymbol{x}, \boldsymbol{x}' \in \mathcal{X}$, we write $\boldsymbol{x} \preceq_{\boldsymbol{\epsilon}} \boldsymbol{x}'$ or $\boldsymbol{F}(\boldsymbol{x}) \preceq_{\boldsymbol{\epsilon}} \boldsymbol{F}(\boldsymbol{x}')$ if $F_1(\boldsymbol{x}) \leq F_1(\boldsymbol{x}') + \epsilon_1$ and $F_2(\boldsymbol{x}) \leq F_2(\boldsymbol{x}') + \epsilon_2$ hold simultaneously. Then, the $\boldsymbol{\epsilon}$-*Pareto front* is defined as:

$$Z_{\boldsymbol{\epsilon}} = \{\boldsymbol{y} \in \mathbb{R}^2 \mid \exists \boldsymbol{y}' \in Z, \boldsymbol{y} \preceq \boldsymbol{y}' \text{ and } \exists \boldsymbol{y}'' \in Z, \boldsymbol{y}'' \preceq_{\boldsymbol{\epsilon}} \boldsymbol{y}\}.$$

We say that the estimated Pareto set $\hat{\Pi}_t$ of the algorithm is an $\boldsymbol{\epsilon}$-accurate Pareto set if the following two conditions are satisfied:

1. $\boldsymbol{F}(\hat{\Pi}_t) \subset Z_{\boldsymbol{\epsilon}}$, where $\boldsymbol{F}(\hat{\Pi}_t) \coloneqq \left\{\boldsymbol{F}(\boldsymbol{x}) \mid \boldsymbol{x} \in \hat{\Pi}_t\right\}$.

2. For any $\boldsymbol{x} \in \Pi$, there is at least one point $\boldsymbol{x}' \in \hat{\Pi}_t$ such that $\boldsymbol{x} \preceq_{\boldsymbol{\epsilon}} \boldsymbol{x}'$.

Intuitively, these conditions indicate that the difference of true Pareto front Z and estimated Pareto front, which is constructed by $\hat{\Pi}_t$, is at most $\boldsymbol{\epsilon}$. We refer to Zuluaga et al. (2016) for more detail explanations of $\boldsymbol{\epsilon}$-Pareto front.

Constrained (Co)-Scenario As an example of constrained optimization scenario, we consider the following problem:

$$\boldsymbol{x}^* = \arg\max_{\boldsymbol{x} \in \mathcal{X}} F_1(\boldsymbol{x}) \text{ s.t. } F_2(\boldsymbol{x}) \geq h,$$

where $h > 0$ is a user-specified known threshold parameter. Moreover, to provide theoretical guarantees, we define an $\boldsymbol{\epsilon}$-accurate solution to be a solution $\hat{\boldsymbol{x}}$ which satisfies $F_1(\hat{\boldsymbol{x}}) \geq F_1(\boldsymbol{x}^*) - \epsilon_1$ and $F_2(\hat{\boldsymbol{x}}) \geq h - \epsilon_2$ for a non-negative vector $\boldsymbol{\epsilon} = (\epsilon_1, \epsilon_2)$.

We emphasize that, although there are many existing studies on multi-task, multi-objective, and constrained BO, these existing methods cannot be directly applied to our problem setups because the objective functions F_1 and F_2 are not observed directly.

3 Proposed Method

First, we explain the basic idea of our proposed algorithms. To handle F_1 and F_2 efficiently, one simple way is to consider the predicted distributions of F_1 and F_2, and apply existing methods. However, it is difficult to handle the predicted distribution of F_2 although f is modeled by a GP. In this paper, we first derive the intervals in which F_1 and F_2 exist with high probability from the confidence bound of f, and construct the algorithm based on these derived intervals. Hereafter, with a slight abuse of notation, we refer to these derived intervals as the confidence bounds of F_1 and F_2.

3.1 Confidence Bounds of Target Functions

The following Lemma 3.1 plays a central role in our proposed methods.

Lemma 3.1. *Let* $\beta_t = \left(\sqrt{2(\gamma_{t-1} + \ln 1/\delta)} + B\right)^2$, *and let*

$$\tilde{l}_t^{(sq)}(\boldsymbol{x}, \boldsymbol{w})$$
$$= \begin{cases} 0, & \tilde{l}_t(\boldsymbol{x}, \boldsymbol{w}) \leq 0 \leq \tilde{u}_t(\boldsymbol{x}, \boldsymbol{w}) \\ \min\left\{\tilde{l}_t^2(\boldsymbol{x}, \boldsymbol{w}), \tilde{u}_t^2(\boldsymbol{x}, \boldsymbol{w})\right\} & \text{otherwise} \end{cases},$$
$$\tilde{u}_t^{(sq)}(\boldsymbol{x}, \boldsymbol{w}) = \max\left\{\tilde{l}_t^2(\boldsymbol{x}, \boldsymbol{w}), \tilde{u}_t^2(\boldsymbol{x}, \boldsymbol{w})\right\}$$

Shogo Iwazaki, Yu Inatsu, Ichiro Takeuchi

where $\tilde{l}_t(\boldsymbol{x}, \boldsymbol{w}) = l_t(\boldsymbol{x}, \boldsymbol{w}) - \mathbb{E}_{\boldsymbol{w}}[u_t(\boldsymbol{x}, \boldsymbol{w})]$ and $\tilde{u}_t(\boldsymbol{x}, \boldsymbol{w}) = u_t(\boldsymbol{x}, \boldsymbol{w}) - \mathbb{E}_{\boldsymbol{w}}[l_t(\boldsymbol{x}, \boldsymbol{w})]$. Then, with probability at least $1 - \delta$, for any $\boldsymbol{x} \in \mathcal{X}$, $t \geq 1$,

$$F_1(\boldsymbol{x}) \in Q_t^{(F_1)}(\boldsymbol{x}) := [l_t^{(F_1)}(\boldsymbol{x}), u_t^{(F_1)}(\boldsymbol{x})],$$
$$F_2(\boldsymbol{x}) \in Q_t^{(F_2)}(\boldsymbol{x}) := [l_t^{(F_2)}(\boldsymbol{x}), u_t^{(F_2)}(\boldsymbol{x})]$$

where

$$l_t^{(F_1)}(\boldsymbol{x}) = \int_\Omega l_t(\boldsymbol{x}, \boldsymbol{w}) p(\boldsymbol{w}) \mathrm{d}\boldsymbol{w},$$

$$u_t^{(F_1)}(\boldsymbol{x}) = \int_\Omega u_t(\boldsymbol{x}, \boldsymbol{w}) p(\boldsymbol{w}) \mathrm{d}\boldsymbol{w},$$

$$l_t^{(F_2)}(\boldsymbol{x}) = -\sqrt{\int_\Omega \tilde{u}_t^{(sq)}(\boldsymbol{x}, \boldsymbol{w}) p(\boldsymbol{w}) \mathrm{d}\boldsymbol{w}},$$

$$u_t^{(F_2)}(\boldsymbol{x}) = -\sqrt{\int_\Omega \tilde{l}_t^{(sq)}(\boldsymbol{x}, \boldsymbol{w}) p(\boldsymbol{w}) \mathrm{d}\boldsymbol{w}}.$$

Lemma 3.1 is derived by considering the intervals where target functions F_1 and F_2 exist when the statement (which occurs with probability $1 - \delta$) in Lemma 2.1 holds. The details of proofs are in Appendix A.

3.2 Algorithms

Multi-task (MT)-Scenario In the multi-task scenario, our algorithm chooses the next input point $\boldsymbol{x}_t$ based on the upper confidence bound (UCB) of the function G in which the lower and the upper bounds are given by

$$l_t^{(G)}(\boldsymbol{x}) = \alpha l_t^{(F_1)}(\boldsymbol{x}) + (1 - \alpha) l_t^{(F_2)}(\boldsymbol{x}),$$
$$u_t^{(G)}(\boldsymbol{x}) = \alpha u_t^{(F_1)}(\boldsymbol{x}) + (1 - \alpha) u_t^{(F_2)}(\boldsymbol{x}).$$

At every step t, the next input point $\boldsymbol{x}_t$ of our algorithm is defined by $\boldsymbol{x}_t = \operatorname{argmax}_{\boldsymbol{x} \in \mathcal{X}} u_t^{(G)}(\boldsymbol{x})$. For theoretical discussion, we define the estimated solution at step t as $\hat{\boldsymbol{x}}_t = \boldsymbol{x}_{\hat{t}}$ with $\hat{t} = \operatorname{argmax}_{t' \in \{1, \dots, t\}} l_{t'}(\boldsymbol{x}_{t'})$. This pessimistic estimated solution is often employed in the other GP-based optimization literatures (e.g., Bogunovic et al., 2018; Kirschner et al., 2020). Hereafter, we call this strategy Multi-Task (MT)-MVA-BO and the pseudo-code is presented in algorithm 1.

Multi-objective (MO)-Scenario From the confidence bounds of F_1 and F_2, we define $\boldsymbol{F}_t^{(\mathrm{opt})}$ and $\boldsymbol{F}_t^{(\mathrm{pes})}$ by $\boldsymbol{F}_t^{(\mathrm{opt})}(\boldsymbol{x}) = \left(u_t^{(F_1)}(\boldsymbol{x}), u_t^{(F_2)}(\boldsymbol{x}) \right)$ and $\boldsymbol{F}_t^{(\mathrm{pes})}(\boldsymbol{x}) = \left(l_t^{(F_1)}(\boldsymbol{x}), l_t^{(F_2)}(\boldsymbol{x}) \right)$, which respectively represent the optimistic and pessimistic predictions of the objective functions at step t. First, based on pessimistic predictions, we define the estimated Pareto set $\hat{\Pi}_t$ at step t by

$$\hat{\Pi}_t = \left\{ \boldsymbol{x} \in \mathcal{X} \mid \forall \boldsymbol{x}' \in E_{t,\boldsymbol{x}}^{(\mathrm{pes})}, \ \boldsymbol{F}_t^{(\mathrm{pes})}(\boldsymbol{x}) \npreceq \boldsymbol{F}_t^{(\mathrm{pes})}(\boldsymbol{x}') \right\},$$

Algorithm 1 Multi-task MVA-BO (MT-MVA-BO)

Input: GP prior $\mathcal{GP}(0, k)$, $\{\beta_t\}_{t \leq T}$, $\alpha \in (0, 1)$.
  for $t = 0$ to T **do**
    Compute $u_t^{(G)}(\boldsymbol{x})$ for any $\boldsymbol{x} \in \mathcal{X}$.
    Choose $\boldsymbol{x}_t = \operatorname{argmax}_{\boldsymbol{x} \in \mathcal{X}} u_t^{(G)}(\boldsymbol{x})$.
    Sample $\boldsymbol{w}_t \sim p(\boldsymbol{w})$.
    Observe $y_t \leftarrow f(\boldsymbol{x}_t, \boldsymbol{w}_t) + \eta_t$.
    Update the GP by adding $((\boldsymbol{x}_t, \boldsymbol{w}_t), y_t)$.
  end for
  $\hat{\boldsymbol{x}}_T = \boldsymbol{x}_{\hat{t}}$ where $\hat{t} = \operatorname{argmax}_{t' \in \{1, \dots, T\}} l_{t'}^{(G)}(\boldsymbol{x}_{t'})$.
Output: $\hat{\boldsymbol{x}}_T$.

---

where $E_{t,\boldsymbol{x}}^{(\mathrm{pes})} = \left\{ \boldsymbol{x}' \in \mathcal{X} \mid \boldsymbol{F}_t^{(\mathrm{pes})}(\boldsymbol{x}) \neq \boldsymbol{F}_t^{(\mathrm{pes})}(\boldsymbol{x}') \right\}$. Furthermore, using $\hat{\Pi}_t$, the potential Pareto set M_t is defined by

$$M_t = \left\{ \boldsymbol{x} \in \mathcal{X} \setminus \hat{\Pi}_t \ \middle| \ \forall \boldsymbol{x}' \in \hat{\Pi}_t, \ \boldsymbol{F}_t^{(\mathrm{opt})}(\boldsymbol{x}) \npreceq_{\boldsymbol{\epsilon}} \boldsymbol{F}_t^{(\mathrm{pes})}(\boldsymbol{x}') \right\}.$$

Here, M_t is the set which excludes the points that are $\boldsymbol{\epsilon}$-dominated by other points with high probability. At every step t, our algorithm chooses $\boldsymbol{x}_t$ based on the uncertainty defined by the confidence bounds of F_1 and F_2. In this paper, we adopt the diameter $\lambda_t(\boldsymbol{x})$ of rectangle $\operatorname{Rect}_t(\boldsymbol{x}) = \left[l_t^{(F_1)}(\boldsymbol{x}), u_t^{(F_1)}(\boldsymbol{x}) \right] \times \left[l_t^{(F_2)}(\boldsymbol{x}), u_t^{(F_2)}(\boldsymbol{x}) \right]$ as the uncertainty of $\boldsymbol{x}$:

$$\lambda_t(\boldsymbol{x}) = \max_{\boldsymbol{y}, \boldsymbol{y}' \in \operatorname{Rect}_t(\boldsymbol{x})} \|\boldsymbol{y} - \boldsymbol{y}'\|_2. \qquad (4)$$

Namely, the next input point $\boldsymbol{x}_t$ is defined by $\boldsymbol{x}_t = \operatorname{argmax}_{\boldsymbol{x} \in M_t \cup \hat{\Pi}_t} \lambda_t(\boldsymbol{x})$ at every step t.

Our proposed algorithm terminates when the estimated Pareto set $\hat{\Pi}_t$ is guaranteed to be an $\boldsymbol{\epsilon}$-Pareto set with high probability. To this end, our algorithm checks the uncertainty set U_t defined by

$$U_t = \Big\{ \boldsymbol{x} \in \hat{\Pi}_t \mid \exists \boldsymbol{x}' \in \hat{\Pi}_t \setminus \{\boldsymbol{x}\},$$
$$\boldsymbol{F}_t^{(\mathrm{pes})}(\boldsymbol{x}) + \boldsymbol{\epsilon} \prec \boldsymbol{F}_t^{(\mathrm{opt})}(\boldsymbol{x}') \Big\}.$$

Here, U_t is the set of points where it is not possible to decide whether it is an $\boldsymbol{\epsilon}$-Pareto solution based on the current confidence bounds. Our algorithm terminates at step t where both $M_t = \emptyset$ and $U_t = \emptyset$ hold. Hereafter, we call this algorithm Multi-Objective (MO)-MVA-BO.

Constrained (Co)-Scenario Let

$$M_t^{(\mathrm{cons})} = \left\{ \boldsymbol{x} \in \mathcal{X} \mid u_t^{(F_2)}(\boldsymbol{x}) \geq h - \epsilon_2 \right\},$$

$$M_t^{(\mathrm{obj})} = \left\{ \boldsymbol{x} \in \mathcal{X} \mid u_t^{(F_1)}(\boldsymbol{x}) \geq \max_{\boldsymbol{x}' \in S_t} l_t^{(F_1)}(\boldsymbol{x}') - \epsilon_1 \right\}.$$

Using these definitions, we define a *potentially* optimal solution set $M_t = M_t^{(\text{cons})} \cap M_t^{(\text{obj})}$. Note that an element in the complement of M_t is not likely to be an ϵ-accurate solution with high probability. In the proposed algorithm, the most uncertain point in the potentially optimal set M_t is selected as the next input point, i.e., $\boldsymbol{x}_t = \text{argmax}_{\boldsymbol{x} \in M_t} \lambda_t(\boldsymbol{x})$, where λ_t is defined in (4). Furthermore, we define the estimated optimal solution as $\hat{\boldsymbol{x}}_t = \text{argmax}_{\boldsymbol{x} \in S_t} l_t^{(F_1)}(\boldsymbol{x})$ where

$$S_t = \left\{ \boldsymbol{x} \in \mathcal{X} \mid l_t^{(F_2)}(\boldsymbol{x}) \geq h - \epsilon_2 \right\}.$$

In order to ensure that $\hat{\boldsymbol{x}}_t$ is an ϵ-accurate solution, the uncertainties of the function values F_1 and F_2 for the potentially optimal solution should be sufficiently small. The algorithm terminates if it satisfies

$$\max_{\boldsymbol{x} \in M_t} \lambda_t(\boldsymbol{x}) \leq \min\{\epsilon_1, \epsilon_2\}.$$

Hereafter, we call this algorithm Constrained (Co)-MVA-BO. Due to the space limitation, we show the pseudo-codes of MO-MVA-BO and Co-MVA-BO in Appendix D.

3.3 Extensions and Practical Considerations

Our algorithms and theoretical analyses can be extended to several different setups.

The details are presented in Appendix B.

3.3.1 Extension to Noisy Input

Our method can be extended to the noisy input setting (Beland and Nair, 2017; Frhlich et al., 2020), in which the input point $\boldsymbol{x}_t$ is fluctuated by noise $\boldsymbol{\xi} \in \Delta$ which follows the known density $p(\boldsymbol{\xi})$ defined over Δ. At every step t, the user chooses $\boldsymbol{x}_t$ and obtains input y_t as $y_t = f(\boldsymbol{x}_t + \boldsymbol{\xi}) + \eta_t$, $\boldsymbol{\xi} \sim p(\boldsymbol{\xi})$. In this setting, we can define F_1 and F_2 based on

$$\mathbb{E}_{\boldsymbol{\xi}}[f(\boldsymbol{x} + \boldsymbol{\xi})] = \int_\Delta f(\boldsymbol{x} + \boldsymbol{\xi}) p(\boldsymbol{\xi}) \mathrm{d}\boldsymbol{\xi},$$

$$\mathbb{V}_{\boldsymbol{\xi}}[f(\boldsymbol{x} + \boldsymbol{\xi})] = \int_\Delta \{f(\boldsymbol{x} + \boldsymbol{\xi}) - \mathbb{E}_{\hat{\boldsymbol{\xi}}}[f(\boldsymbol{x} + \hat{\boldsymbol{\xi}})]\}^2 p(\boldsymbol{\xi}) \mathrm{d}\boldsymbol{\xi}.$$

We can apply the same algorithms as those in section 3.2 by constructing the confidence bounds via a way similar to that in section 3.1.

3.3.2 Simulator-Based Experiment

In some applications, it is reasonable to assume that the environmental variable $\boldsymbol{w}$ randomly varies according to $p(\boldsymbol{w})$ only in the *usage phase*, while it is controllable during the *optimization phase*. Such scenarios have often been considered in similar studies reported

in the BO literature under uncertain environment (Beland and Nair, 2017; Toscano-Palmerin and Frazier, 2018; Kirschner et al., 2020; Nguyen et al., 2020). Our algorithms and theories can be extended to such setup by choosing $\boldsymbol{w}_t = \text{argmax}_{\boldsymbol{w} \in \Omega} \sigma_{t-1}(\boldsymbol{x}_t, \boldsymbol{w})$ after the selection of $\boldsymbol{x}_t$.

4 Theoretical Results

In this section, we show the theoretical results of the proposed algorithms. The proofs are presented in Appendix A. Note that although our proposed algorithms inherent to the existing confidence bound-based methods (Srinivas et al., 2010; Sui et al., 2015; Zuluaga et al., 2016), our theoretical guarantees are non-trivial because the theoretical property of our derived confidence bounds is different from those in existing works.

The following Theorem 4.1 provides the convergence property of MT-MVA-BO.

Theorem 4.1. *Fix positive definite kernel k, and assume $f \in \mathcal{H}_k$ with $\|f\|_{\mathcal{H}_k} \leq B$. Let $\delta \in (0, 1)$ and $\epsilon > 0$, and set β_t according to $\beta_t = \left(\sqrt{2(\gamma_{t-1} + \ln(3/\delta))} + B \right)^2$ at every step t. Furthermore, for any $t \geq 1$, define $\hat{\boldsymbol{x}}_t$ by $\hat{\boldsymbol{x}}_t = \boldsymbol{x}_{\hat{t}}$ with $\hat{t} = \text{argmax}_{t' \in \{1, \ldots, t\}} l_{t'}^{(G)}(\boldsymbol{x}_{t'})$. When applying MT-MVA-BO under the above conditions, with probability at least $1 - \delta$, $\hat{\boldsymbol{x}}_T$ is an ϵ-accurate solution, where T is the smallest positive integer which satisfies $R_T/T \geq \epsilon$ with*

$$R_T = (1 - \alpha) \sqrt{2T \tilde{B} \beta_T^{1/2} \left(\sqrt{8T C_1 \gamma_T} + 2C_2 \right) + 5T \beta_T C_T}$$
$$+ \alpha \beta_T^{1/2} \left(\sqrt{2T C_1 \gamma_T} + C_2 \right). \tag{5}$$

Here, $\tilde{B} = \max_{(\boldsymbol{x}, \boldsymbol{w}) \in (\mathcal{X} \times \Omega)} |f(\boldsymbol{x}, \boldsymbol{w}) - \mathbb{E}_{\boldsymbol{w}}[f(\boldsymbol{x}, \boldsymbol{w})]|$ and $C_1 = \frac{16}{\log(1 + \sigma^{-2})}, C_2 = 16 \log \frac{18}{\delta}, C_T = C_1 \gamma_T + 2C_2$.

The second term of R_T is induced from confidence bound of F_1. When $\alpha = 1$, we can find that $R_T = \mathcal{O}(\sqrt{T \beta_T \gamma_T})$ and it recovers the result of the existing result which only focuses on the maximization of F_1 (Kirschner et al., 2020) [4].

The first term of R_T is specific to our setting. This is induced from the confidence bound of F_2, and depends on the complexity parameter $\tilde{B}$ which characterizes the variation of function $f(\boldsymbol{x}, \boldsymbol{w})$ around its expectation. Noting that $k((\boldsymbol{x}, \boldsymbol{w}), (\boldsymbol{x}, \boldsymbol{w})) \leq 1$ holds for any $(\boldsymbol{x}, \boldsymbol{w}) \in \mathcal{X} \times \Omega$, $f(\boldsymbol{x}, \boldsymbol{w})$ is bounded as $f(\boldsymbol{x}, \boldsymbol{w}) =$

---

[4] Although Kirschner et al. (2020) considers the distributionally robust setting of maximization of F_1, their algorithm can be applied to the non-robust setting by considering the singleton set of the distribution.

$\langle f, k((\boldsymbol{x}, \boldsymbol{w}), \cdot) \rangle_{\mathcal{H}_k} \leq B$ for any $(\boldsymbol{x}, \boldsymbol{w}) \in \mathcal{X} \times \Omega$ by applying the Schwarz's inequality. Therefore, we can find that the parameter $\tilde{B}$ is roughly bounded as $\tilde{B} \leq 2B$.

Furthermore, we can obtain more explicit form of Theorem 4.1 by substituting bounds on γ_T. For example, $\gamma_T = \mathcal{O}((\log T)^{d_1 + d_2 + 1})$ in Gaussian kernel. In this case, R_T becomes sub-linear (i.e. $\lim_{T \to \infty} R_T / T = 0$). Hence, for arbitrarily small $\epsilon > 0$, Theorem 4.1 guarantees that MT-MVA-BO returns an ϵ-accurate solution within finite steps with high probability.

Finally, we present the similar convergence results for MO-MVA-BO and Co-MVA-BO in Theorem 4.2 and 4.3, respectively.

Theorem 4.2. *Fix positive definite kernel k, and assume $f \in \mathcal{H}_k$ with $\|f\|_{\mathcal{H}_k} \leq B$. Let $\delta \in (0, 1)$ and $\epsilon > 0$, and set β_t according to $\beta_t = \left(\sqrt{2(\gamma_{t-1} + \ln(3/\delta))} + B \right)^2$ at every step t. When applying MO-MVA-BO under the above conditions, the following 1. and 2. hold with probability at least $1 - \delta$:*

1. *The algorithm terminates at most step T where T is the smallest positive integer that satisfies the following inequality:*

$$\sqrt{4 T \tilde{B} \beta_T^{1/2} \left(\sqrt{2 T C_1 \gamma_T} + C_2 \right) + 5 T \beta_T C_T} \quad (6)$$
$$+ \beta_T^{1/2} \left(\sqrt{2 T C_1 \gamma_T} + C_2 \right) \leq T \min\{\epsilon_1, \epsilon_2\}.$$

2. *When the algorithm terminates, estimated Pareto set $\hat{\Pi}_t$ is an $\boldsymbol{\epsilon}$-accurate Pareto set.*

Theorem 4.3. *Let k be a positive-definite kernel, and let $f \in \mathcal{H}_k$ with $\|f\|_{\mathcal{H}_k} \leq B$. Also let $\delta \in (0, 1)$ and $\epsilon_1 > 0$, $\epsilon_2 > 0$, and define $\beta_t = \left(\sqrt{2(\gamma_{t-1} + \ln(3/\delta))} + B \right)^2$. Then, with probability at least $1 - \delta$, the following 1. and 2. hold:*

1. *Co-MVA-BO algorithm in §3 terminates after at most T iterations, where T is the smallest positive integer satisfying*

$$\sqrt{2 T \tilde{B} \beta_T^{1/2} \left\{ \sqrt{8 T C_1 \gamma_T} + 2 C_2 \right\} + 5 T \beta_T C_T} \quad (7)$$
$$+ \beta_T^{1/2} \left\{ \sqrt{2 T C_1 \gamma_T} + C_2 \right\} \leq T \min\{\epsilon_1, \epsilon_2\}.$$

2. *If $\boldsymbol{x}^*$ exists, then $S_{t'} \neq \emptyset$ at the termination step $t' \leq T$. Moreover, $\hat{\boldsymbol{x}}_{t'} = \operatorname{argmax}_{\boldsymbol{x} \in S_{t'}} l_t^{(F_1)}(\boldsymbol{x})$ is an ϵ-accurate solution.*

5 Numerical Experiments

We conducted intensive numerical experiments on a variety of artificial and real datasets. Due to the space

limitation, we only show a part of the results. See Appendix E for more experimental results and detailed experimental setups. As the common baselines in the three scenarios, we adopted random sampling (RS) and uncertainty sampling (US). RS chooses $\boldsymbol{x}_t$ from $\mathcal{X}$ uniformly at random, and US chooses $\boldsymbol{x}_t$ such that it achieves the largest average posterior variance.

In the multi-task scenario, we computed the regret, $G(\boldsymbol{x}^*) - G(\hat{\boldsymbol{x}}_t)$, at every step t, where $\boldsymbol{x}_t$ is the estimated solution defined by the algorithms. We defined $\hat{\boldsymbol{x}}_t$ as $\hat{\boldsymbol{x}}_t = \operatorname{argmax}_{t'=1,\ldots,t} l_t^{(G)}(\boldsymbol{x}_{t'})$ [5] in RS, US, and proposed method (MT-MVA-BO). To show the effect of difference of objective functions, we also considered two methods BQOUCB and BO-VO. The former is the method designed to maximize F_1, and this method is also considered for comparison in existing BO studies under uncertainty (Nguyen et al., 2020; Kirschner et al., 2020). The latter is the variant of our method corresponding to the case of $\alpha = 0$. These methods choose $\boldsymbol{x}_t$ as the maximizing point of $u_t^{(F_1)}(\boldsymbol{x})$ and $u_t^{(F_2)}(\boldsymbol{x})$ respectively. In addition, estimated solution $\hat{\boldsymbol{x}}_t$ is defined by $\hat{\boldsymbol{x}}_t = \operatorname{argmax}_{t'=1,\ldots,t} l_t^{(F_1)}(\boldsymbol{x}_{t'})$ and $\hat{\boldsymbol{x}}_t = \operatorname{argmax}_{t'=1,\ldots,t} l_t^{(F_2)}(\boldsymbol{x}_{t'})$, respectively. We also compared with the adaptive versions of these methods ADA-BQOUCB and ADA-BO-VO, which choose $\boldsymbol{x}_t$ in the same way as BQOUCB and BO-VO, but the estimated solutions are defined as $\hat{\boldsymbol{x}}_t = \operatorname{argmax}_{t'=1,\ldots,t} l_t^{(G)}(\boldsymbol{x}_{t'})$. We set α so that maximums of the mean function F_1, the variance function F_2 and the target function G become different. The values of α that we used in each experiments are in appendix.

In the multi-objective scenario, we adopted RS and US for comparison. We computed the gap of hypervolume (Emmerich, 2005), $\mathrm{HV} - \hat{\mathrm{HV}}_t$ to measure the performance, where HV and $\hat{\mathrm{HV}}_t$ denote the hypervolumes computed based on the true Pareto set Π and the estimated Pareto set $\hat{\Pi}_t$, respectively.

In the constrained optimization scenario, we adopted RS, US, and BQOUCB for comparison. We defined $\hat{\boldsymbol{x}}_t = \operatorname{argmax}_{\boldsymbol{x} \in S_t} l_t^{(F_1)}(\boldsymbol{x})$ in RS and US, whereas $\hat{\boldsymbol{x}}_t = \operatorname{argmax}_{\boldsymbol{x} \in \mathcal{X}} l_t^{(F_1)}(\boldsymbol{x})$ in BQOUCB. We considered ADA-BQO-UCB, an adaptive version of BQOUCB, which chooses the next point in the same way as what BQOUCB does, but $\hat{\boldsymbol{x}}_t$ is defined as $\hat{\boldsymbol{x}}_t = \operatorname{argmax}_{\boldsymbol{x} \in S_t} l_t^{(F_1)}(\boldsymbol{x})$. To measure performances, we used the utility gap measure which is commonly used as a performance measure in constrained BO (Hernández-Lobato et al., 2016). As a performance measure, at every step t, we report the

---

[5] Note that this definition is slightly different from that of Theorem 4.1. As described by Bogunovic et al. (2018), this definition is more suitable than that of Theorem 4.1 when the kernel hyperparameters are updated online.

utility gap defined as $F_1(\boldsymbol{x}^*) - F_1(\hat{\boldsymbol{x}}_t)$ if $F_2(\hat{\boldsymbol{x}}_t) \geq h$, whereas $F_1(\boldsymbol{x}^*) - \min_{\boldsymbol{x} \in \mathcal{X}} F_1(\boldsymbol{x})$ otherwise.

GP Test Functions First, we conducted experiments with true oracle functions f generated from 2D GP prior. We divided $[-1, 1]^2$ into 25 uniformly spaced grid points in each dimension and generated the sample path from the GP prior. Then, we created the GP model with these grid points and set the true oracle function as its GP posterior mean. Here, we created 50 sample paths from different seeds, and conducted 10 runs for each function and report the average performance of a total of 500 experiments. To create a GP sample path, we used the Gaussian kernel $k((\boldsymbol{x}, \boldsymbol{w}), (\boldsymbol{x}', \boldsymbol{w}')) = \sigma_{\text{ker}}^2 \exp((\|\boldsymbol{x} - \boldsymbol{x}'\|_2^2 + \|\boldsymbol{w} - \boldsymbol{w}'\|_2^2)/(2l^2))$ with $\sigma_{\text{ker}} = 1, l = 0.25$ and assume that it is known in all the algorithms. The noise variance was set to be $\sigma^2 = 10^{-4}$. The domain spaces $\mathcal{X}$ and Ω are set to be 100 grid points evenly allocated in $[-1, 1]$. The density was set to be $p(w) = \sum_{w \in \Omega} \phi(w)/Z$, $Z = \sum_{w \in \Omega} \phi(w)$ where ϕ is p.d.f. of standard normal distribution.

Benchmark Functions We also conducted experiments with 6 benchmark functions commonly used in BO study. Due to the space limitation, we only show the results of 3D Rosenbrock function. First, we scaled the input domain to $[-1, 1]^3$ and divided it with 100 grid points in each dimension. Here, we set the first two dimensions as $\mathcal{X}$ and the remaining one dimension as Ω. Furthermore, we set $p(w)$ in the same way as the experiments with GP test functions. We used ARD Gaussian kernel $k((\boldsymbol{x}, \boldsymbol{w}), (\boldsymbol{x}', \boldsymbol{w}')) = \sigma_{\text{ker}}^2 \exp(\sum_{i=1}^{d_1} (\boldsymbol{x}_i - \boldsymbol{x}'_i)^2 / 2l_i^{(x)2} + \sum_{j=1}^{d_2} (\boldsymbol{w}_j - \boldsymbol{w}'_j)^2 / 2l_j^{(w)2})$. Unlike the experiments with GP test functions, we assumed that the hyperparameters are unknown, and they are estimated by maximizing the marginal likelihood at every 10 step in the algorithms. We set the noise variance as $\sigma^2 = 10^{-4}$ and report the average performance of 50 simulations with different seeds.

Real-data We applied the proposed methods to two real-world problems: *Portfolio optimization problem* and *Newsvendor problem under dynamic consumer substitution* (Mahajan and Van Ryzin, 2001). The goal of the former problem is to optimize hyperparamters of a trading strategy under uncertainty of market conditions, while the goal of the latter problem is to optimize the initial inventory levels under uncertainty of customer behaviors. In the former problem, the control parameter $\boldsymbol{x}$ corresponds to the risk and trade aversion parameters, and the holding cost multiplier, respectively. The environmental parameters $\boldsymbol{w}$ are the bid-ask spread and the borrow cost, which are assumed

to be uniformly distributed over certain ranges. In the latter problem, the control parameter $\boldsymbol{x}$ and $\boldsymbol{w}$ respectively correspond to the initial inventory level of products and the uncertain purchasing behaviors of customers, which follow mutually independent Gamma distributions. These problems are also considered in existing BO studies under uncertainty environment (Toscano-Palmerin and Frazier, 2018; Cakmak et al., 2020). As in these previous studies (Toscano-Palmerin and Frazier, 2018; Cakmak et al., 2020), we conducted the experiments in the simulator-based setting described in section 3.3.2. The average performances of 30 simulations with different seeds are reported.

Results Figure 2 shows the results of a GP test function, a benchmark data (Rosenbrock), and two real data (Portfolio and Newsvendor). In all the datasets and all the three scenarios, the proposed methods MVA-BO (in red color) showed better or at least comparable performances than other methods. In the experiments of the multi-task and constraint optimization scenario, we also confirmed that the regrets of `BQOUCB`, `BO-VO`, `ADA-BQOUCB`, and `ADA-BO-VO` stop decreasing at an early stage. Note that these are reasonable results because target functions of these methods are inconsistent with our settings.

6 Conclusion

We introduced mean-variance analysis within the context of Bayesian Optimization under uncertainty. We developed algorithms for multi-task, multi-objective and constrained optimization scenarios, analyzed their convergence properties, and demonstrated their effectiveness through numerical experiments.
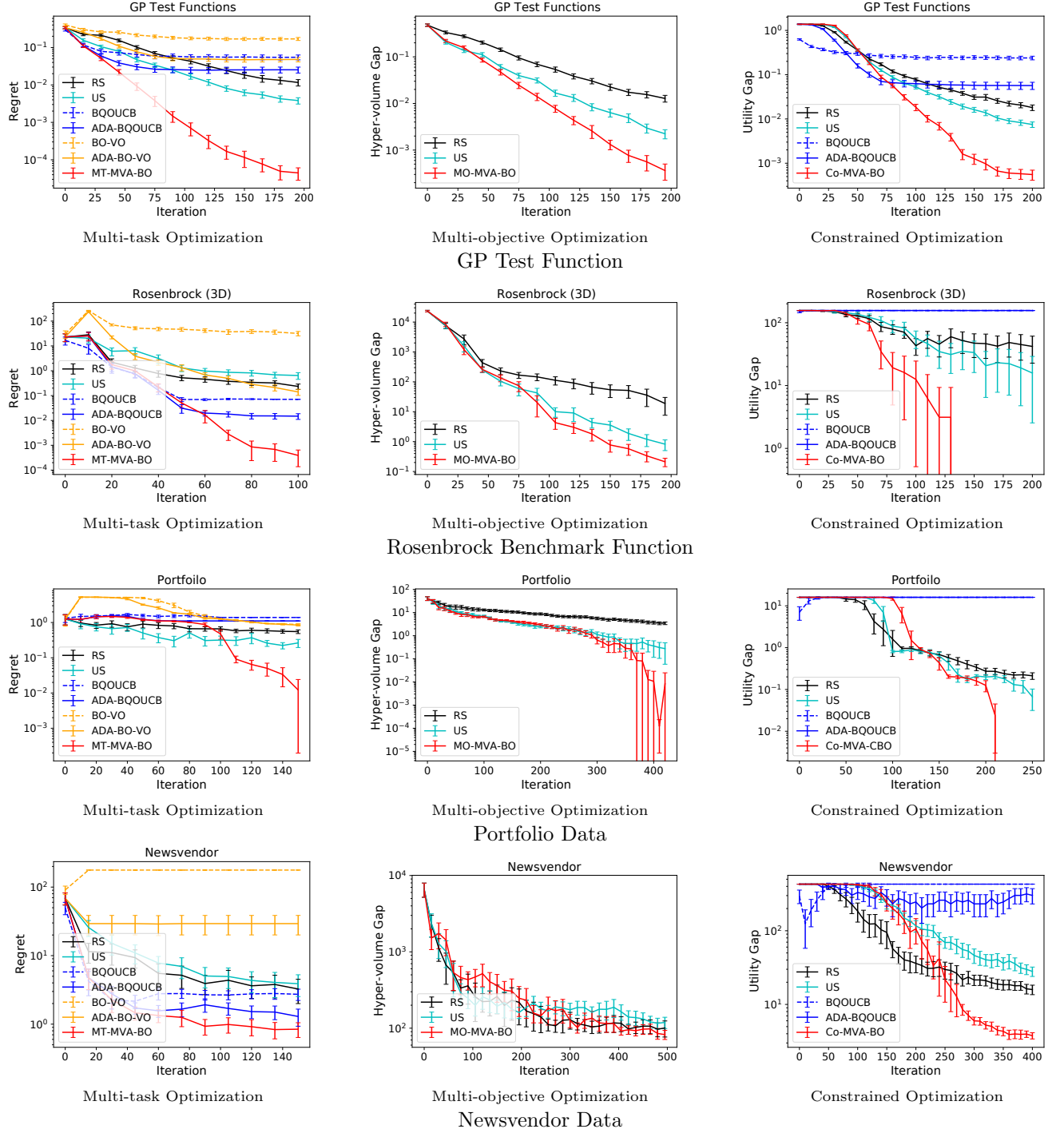
Acknowledgement

Figure 2: Experimental results on two artificial datasets (GP test function and Rosenbrock function) and two real datasets (Portfolio and Newsvendor) in multi-task (left), multi-objective (center) and constrained (right) optimization scenarios. Average performances and error bars ($2 \times$ standard error) over multiple trials are plotted for each method in each setup. In almost all the datasets and scenarios, the proposed MVA-BO methods (MT-MVA-BO, MO-MVA-BO, Co-MVA-BO in red colors) showed better performances than other methods. More results on other datasets and other problem setups are presented in Appendix E.

References

Yasin Abbasi-Yadkori. Online learning for linearly parametrized control problems. 2013.

Gordon J Alexander and Alexandre M Baptista. Economic implications of using a mean-var model for portfolio selection: A comparison with mean-variance analysis. *Journal of Economic Dynamics and Control*, 26(7-8):1159–1193, 2002.

Justin J Beland and Prasanth B Nair. Bayesian optimization under uncertainty. In *NIPS BayesOpt 2017 workshop*, 2017.

Aharon Ben-Tal and Arkadi Nemirovski. Robust optimization–methodology and applications. *Mathematical programming*, 92(3):453–480, 2002.

Aharon Ben-Tal, Laurent El Ghaoui, and Arkadi Nemirovski. *Robust optimization*, volume 28. Princeton University Press, 2009.

Hans-Georg Beyer and Bernhard Sendhoff. Robust optimization–a comprehensive survey. *Computer methods in applied mechanics and engineering*, 196 (33-34):3190–3218, 2007.

Ilija Bogunovic, Jonathan Scarlett, Stefanie Jegelka, and Volkan Cevher. Adversarially robust optimization with Gaussian processes. In *Advances in neural information processing systems*, pages 5760–5770, 2018.

Ilija Bogunovic, Andreas Krause, and Jonathan Scarlett. Corruption-tolerant Gaussian process bandit optimization. In *The 23rd International Conference on Artificial Intelligence and Statistics, AISTATS 2020*, volume 108 of *Proceedings of Machine Learning Research*, pages 1071–1081, 2020.

Sait Cakmak, Raul Astudillo, Peter Frazier, and Enlu Zhou. Bayesian optimization of risk measures. *arXiv preprint arXiv:2007.05554*, 2020.

Sayak Ray Chowdhury and Aditya Gopalan. On kernelized multi-armed bandits. In *Proceedings of the 34th International Conference on Machine Learning*, volume 70 of *Proceedings of Machine Learning Research*, pages 844–853, International Convention Centre, Sydney, Australia, 06–11 Aug 2017. URL http://proceedings.mlr.press/v70/chowdhury17a.html.

Michael Emmerich. Single-and multi-objective evolutionary design optimization assisted by Gaussian random field metamodels. *Dissertation, LS11, FB Informatik, Universität Dortmund, Germany*, 2005.

Frank J Fabozzi, Petter N Kolm, Dessislava A Pachamanova, and Sergio M Focardi. Robust portfolio optimization. *The Journal of portfolio management*, 33(3):40–48, 2007.

Lukas Frhlich, Edgar Klenske, Julia Vinogradska, Christian Daniel, and Melanie Zeilinger. Noisy-input entropy search for efficient robust Bayesian optimization. In *Proceedings of the Twenty Third International Conference on Artificial Intelligence and Statistics*, volume 108 of *Proceedings of Machine Learning Research*, pages 2262–2272, Online, 26–28 Aug 2020. URL http://proceedings.mlr.press/v108/frohlich20a.html.

Jacob R Gardner, Matt J Kusner, Zhixiang Eddie Xu, Kilian Q Weinberger, and John P Cunningham. Bayesian optimization with inequality constraints. In *ICML*, volume 2014, pages 937–945, 2014.

Michael A. Gelbart, Jasper Snoek, and Ryan P. Adams. Bayesian optimization with unknown constraints. In *Proceedings of the Thirtieth Conference on Uncertainty in Artificial Intelligence*, UAI'14, page 250259, Arlington, Virginia, USA, 2014. AUAI Press. ISBN 9780974903910.

José Miguel Hernández-Lobato, Michael A Gelbart, Ryan P Adams, Matthew W Hoffman, and Zoubin Ghahramani. A general framework for constrained Bayesian optimization using information-based search. *The Journal of Machine Learning Research*, 17(1):5549–5601, 2016.

Yu Inatsu, Shogo Iwazaki, and Ichiro Takeuchi. Active learning for distributionally robust level-set estimation. *arXiv preprint arXiv:2102.04000*, 2021.

Shogo Iwazaki, Yu Inatsu, and Ichiro Takeuchi. Bayesian experimental design for finding reliable level set under input uncertainty. *IEEE Access*, 8: 203982–203993, 2020a. doi: 10.1109/ACCESS.2020. 3036863.

Shogo Iwazaki, Yu Inatsu, and Ichiro Takeuchi. Bayesian quadrature optimization for probability threshold robustness measure. *arXiv preprint arXiv:2006.11986*, 2020b.

Michael C Keeley and Frederick T Furlong. A reexamination of mean-variance analysis of bank capital regulation. *Journal of Banking & Finance*, 14(1): 69–84, 1990.

Johannes Kirschner, Ilija Bogunovic, Stefanie Jegelka, and Andreas Krause. Distributionally robust Bayesian optimization. In *The 23rd International Conference on Artificial Intelligence and Statistics, AISTATS 2020, 26-28 August 2020, Online [Palermo, Sicily, Italy]*, volume 108 of *Proceedings of Machine Learning Research*, pages 2174–2184, 2020. URL http://proceedings.mlr.press/v108/kirschner20a.html.

Siddharth Mahajan and Garrett Van Ryzin. Stocking retail assortments under dynamic consumer substitution. *Operations Research*, 49(3):334–351, 2001.

Harry Markowitz. Portfolio selection. *Journal of Finance*, 7(1):77–91, 1952.

Harry M Markowitz and G Peter Todd. *Mean-variance analysis in portfolio choice and capital markets*, volume 66. John Wiley & Sons, 2000.

Thanh Nguyen, Sunil Gupta, Huong Ha, Santu Rana, and Svetha Venkatesh. Distributionally robust Bayesian quadrature optimization. In *Proceedings of the Twenty Third International Conference on Artificial Intelligence and Statistics*, volume 108 of *Proceedings of Machine Learning Research*, pages 1921–1931, Online, 26–28 Aug 2020. URL `http://proceedings.mlr.press/v108/nguyen20a.html`.

Anthony O'Hagan. Bayes–hermite quadrature. *Journal of statistical planning and inference*, 29(3):245–260, 1991.

Carl Edward Rasmussen and Christopher K. I. Williams. *Gaussian Processes for Machine Learning*. MIT Press, 2006.

Alexander Schied. Risk measures and robust optimization problems. *Stochastic Models*, 22(4):753–831, 2006.

Niranjan Srinivas, Andreas Krause, Sham M. Kakade, and Matthias W. Seeger. Gaussian process optimization in the bandit setting: No regret and experimental design. In *Proceedings of the 27th International Conference on Machine Learning (ICML-10), June 21-24, 2010, Haifa, Israel*, pages 1015–1022, 2010. URL `https://icml.cc/Conferences/2010/papers/422.pdf`.

Yanan Sui, Alkis Gotovos, Joel Burdick, and Andreas Krause. Safe exploration for optimization with Gaussian processes. In *International Conference on Machine Learning*, pages 997–1005, 2015.

Shinya Suzuki, Shion Takeno, Tomoyuki Tamura, Kazuki Shitara, and Masayuki Karasuyama. Multi-objective Bayesian optimization using Pareto-frontier entropy. In *Proceedings of Machine Learning and Systems 2020*, pages 10841–10850. 2020.

Kevin Swersky, Jasper Snoek, and Ryan P Adams. Multi-task Bayesian optimization. In *Advances in neural information processing systems*, pages 2004–2012, 2013.

Shion Takeno, Tomoyuki Tamura, Kazuki Shitara, and Masayuki Karasuyama. Sequential- and parallel-constrained max-value entropy search via information lower bound. *arXiv preprint arXiv:2102.09788*, 2021.

Saul Toscano-Palmerin and Peter I. Frazier. Bayesian optimization with expensive integrands. *CoRR*, abs/1803.08661, 2018. URL `http://arxiv.org/abs/1803.08661`.

Marcela Zuluaga, Andreas Krause, and Markus Püschel. e-pal: An active learning approach to the multi-objective optimization problem. *Journal of Machine Learning Research*, 17(104):1–32, 2016. URL `http://jmlr.org/papers/v17/15-047.html`.